

# Image stylization using anisotropic reaction diffusion

Ming-Te Chi · Wei-Ching Liu · Shu-Hsuan Hsu

Received: date / Accepted: date

**Abstract** Image stylization refers to the process of converting input images to a specific representation that enhances image content using several designed patterns. The critical steps to a successful image stylization are the design of patterns and arrangements. However, only skilled artists master such tasks because these tasks are challenging for most users. In this paper, a novel image stylization system based on anisotropic reaction diffusion is proposed to facilitate pattern generation and stylized image design. The system begins with self-organized patterns generated by reaction diffusion. To extend the style of reaction diffusion, the proposed method involves using a set of modifications of anisotropic diffusion to deform shape and introducing a flow field to guide pattern arrangement. A pattern picker is proposed to facilitate the pattern selection from these modifications. In the post-process step, a new thresholding and color mapping method is introduced to refine the sizes, densities, and colors of patterns. From the experimental results and a user study, several image stylizations, including paper-cut, stylized halftone, and motion illusion, are generated by using our method, demonstrating the feasibility and flexibility of the proposed system.

**Keywords** image stylization · reaction diffusion · pattern generation

---

Ming-Te Chi  
National Chengchi University.  
E-mail: mtchi@cs.nccu.edu.tw

Wei-Ching Liu and Shu-Hsuan Hsu  
National Chengchi University.

## 1 Introduction

The rapid development of digital authoring tool has expanded in scope to the creation of artworks featuring new styles. An easily controllable and diversified authoring tool can improve efficiency and facilitate creativity among artists. Image stylization is an essential nonphotorealistic rendering (NPR) technique that can be used to modify the style of input images, enhance image features, and express specific visual cues. This technique mainly depends on the generalization of stylized patterns, which involve pattern shapes and spatial distributions.

Biological patterns, such as leopard spots and zebra stripes, can be generated using the technique of reaction diffusion. A reaction diffusion system is a mathematical model used to describe the interaction of multiple chemicals. Many studies [11, 17, 19] have proposed the use of reaction diffusion to pattern generation. Although the methods based on reaction diffusion can generate complex patterns through simple equations, the dynamic generating process and the lack of controllability on details make generating the desired results difficult to amateur users. Therefore, the core concept of the proposed system is to simplify the parameter adjustment though a pattern picker and guide the reaction diffusion system along a flow direction to generate a stylized pattern distribution that can preserve and enhance the features of input images.

An image stylization method is proposed in this study to generate images with various styles including paper-cut, halftone, and flow styles. To create quality images that depict salient features, the created patterns require distinct primitive placements and geometric shapes. For instance, the images of the paper-cut style can be considered as a collage of several ge-

ometric patterns. Therefore, the creation of these images requires a thresholding process. By contrast, for the halftone images, the tone variations are realized by arranging small geometric primitives. Because of the variety of primitives, the recreated images are vivid and expressive. Flow field is also another image characteristic. Determining how to place stylized primitives to depict flow is crucial in flow visualization and image stylization. Furthermore, a flexible pattern selection and adjustment tool are required in a stylization system that can aid users to yield a compelling result. In this study, several approaches are proposed to make an image stylization system meet these requirements. Compared with related methods, our study provides the following contributions:

- The combination of flow fields with a reaction diffusion model enables our method to preserve not only the edge features and tones but also the flow features of the input images.
- A pattern guide image is generated to summarize the pattern style. Users can intuitively select their desired patterns and create stylized results.
- The post-processing methods are proposed to enrich the tone and flow feature by thresholding and color mapping.

The remainder of this paper is organized as follows. Section 2 reviews the related work. Section 3 presents the proposed approaches. Section 4 discusses the experimental results, and Section 5 presents the conclusions, limitations, and future work.

## 2 Related work

### 2.1 Reaction diffusion

Numerous studies on pattern generation and texture synthesis have been inspired by reaction diffusion system. Reaction diffusion describes the reaction of two chemical substances in morphogens, which can be used to generate biological patterns. Witkin and Kass [19] and Turk [17] applied the reaction diffusion system to surface texture, which generated various types of spot and stripe pattern. McGraw [11] introduced tensor to represent high-order diffusion displacement in order to generate inorganic patterns. Wan et al. [18] adopted stripe pattern from reaction diffusion to create maze. The additional anisotropic diffusion term extended the range of patterns and enabled control over resulting patterns. However, designing stylized images using reaction diffusion has remained difficult.

Few approaches have addressed reaction diffusion by using flow fields. Sanderson et al. [14] proposed an ad-

justed anisotropic diffusion for deformed spot patterns to visualize a flow field. Kim and Lin [6] introduced an anisotropy-embedding function and an advection term to expand the range of patterns. We extended this approach to implement anisotropic designs in a flow field to enhance shaping and color mapping to provide more effective flow visualizations.

### 2.2 Image stylization

Numerous researchers have attempted to implement the principles and techniques of various kinds of arts in computer graphics. Xu et al. [21] presented a paper-cut style generated from bitonal images under geometric connectivity constraints. Xu et al. [20] introduced a novel concept to depict continuous-tone images by applying optimized thresholding to bitonal images while retaining salient features. This bitonal approach can also be used to control abstraction in image rendering. Zang et al. [22] introduced a preprocessing step method to preserve the feature of image and simulate the image enhancement by artist.

Among the rich and diverse image stylization techniques, flow-based stylization methods are reviewed here. To automatically generate the flow field from the input image, Kang et al. [4] proposed a flow-generating method that involves transferring the gradients of the input image to flow vectors and drawing coherent lines by using the flow-based difference of the Gaussian filter. Bousseau et al. proposed video water colorization [2]. They adapted texture advection along the optical flow to maintain the coherence of the watercolor style. Kyprianidis et al. [7] and Kang et al. [5] have generated flow fields based on the edge tangent flow (ETF) from source images. The use of ETF strengthens the continuity of stylized lines and ensures that stylized images are smoother compared with those generated through traditional methods. Kyprianidis et al. [8] proposed stylized abstraction based on directional shock filtering. Lee et al. [9] exploited a flow field to develop a texture-transfer method. The method introduced by Li et al. [10] enables users to design geometric patterns by applying field-guided shape grammars. In addition to producing basic designs, resulting patterns can be ornamented with the flow field with minimal distortion. Son et al. proposed a stippling algorithm [15] that can effectively maintain the dot distribution in the application of the flow field. This method can be used to reproduce the tones and features of input images. Direction information is not only useful for stylization, but also useful for preserve the detail. Steidl and Teuber [16] proposed an anisotropic smoothing method in image restoration.

### 3 Method

#### 3.1 Reaction diffusion

A Gray-Scott reaction-diffusion is one of common models of reaction diffusion which given by

$$\begin{aligned}\frac{\partial A}{\partial t} &= D_A \nabla^2 A - AB^2 + F(1 - A) \\ \frac{\partial B}{\partial t} &= D_B \nabla^2 B + AB^2 - (F + k)B,\end{aligned}\quad (1)$$

where  $A$  and  $B$  denote the density field of two chemicals. The equation describes the change in density field of  $A$  and  $B$  over time. The first term is the diffusion term, in which  $D_A$  and  $D_B$  denote the diffusion rates of  $A$  and  $B$ , and  $\nabla^2 A$  is the Laplacian of  $A$ . The second term is used to describe the reaction. The reaction equation shows that one unit of  $A$  and two units of  $B$  will become to three units of  $B$ . In the third term,  $F$  and  $k$  are the parameters specified by the user to control the replenishment rate of  $A$  and the diminishment rate of  $B$ . ( $F + k$ ) is used to guarantee the decreasing speed of  $B$ , which is faster than the production speed of  $A$ . In this study, the distribution of  $A$  is used as a pattern arrangement. The nature of reaction diffusion makes producing self-organized patterns with non-regular distribution easy. This idea is different from the related works on pattern arrangement and image stylization.

The relationship between pattern styles and the reaction diffusion model was studied by Pearson [12]. He illustrated the parameterizations of the Gray-Scott model and classified the patterns into several types. Figure 1 shows the types of stable patterns and their corresponding parameter spaces. The result of stable pattern is similar and not exactly the same under the different initial condition and running steps. This property enriches the stylization and makes the pattern more naturally. The proposed method utilizes these stable stylized patterns and their extended patterns to yield a great variety of stylization.

#### 3.2 Anisotropic diffusion

Anisotropic diffusion enables flexible adjustment in deformation and rotation in the step of pattern generation. We applied the anisotropic diffusion term as

$$\begin{aligned}\frac{\partial A}{\partial t} &= D_A(\nabla \cdot a(\theta_{V, \nabla A}) \nabla A) - AB^2 + F(1 - A) \\ \frac{\partial B}{\partial t} &= D_B(\nabla \cdot a(\theta_{V, \nabla B}) \nabla B) + AB^2 - (F + k)B,\end{aligned}\quad (2)$$

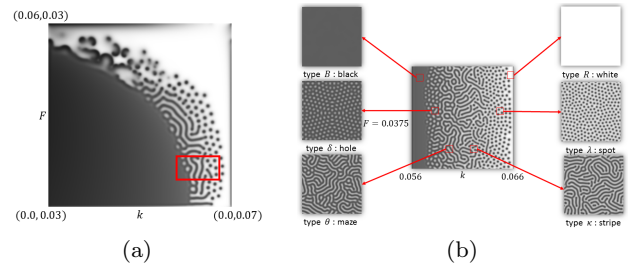


**Fig. 1** Parameterizations in the Gray-Scott model. (a) Various pattern types in the domain of parameters  $F$  and  $k$ . (b) Cloud-up view of the red box in (a). The stable patterns were classified by [12].

where  $a(\theta)$  denotes the anisotropic function, and  $\theta_{V, \nabla A}$  is the angle between direction vector of in the flow field  $V$  and gradient vector in the gradient field of  $A$ . The generated pattern is then deformed according to the anisotropic function and rotated along the flow field. For example, a spot pattern is deformed to a spindle pattern in Figure 2 (b), and the pattern orientation follows the flow field. However, each spot maintains an equal distance to neighboring spots because of the fixed and regular Laplacian kernel specified in Eq. 2. The flow-guided diffusion in our system is adopted to correlate the arrangement into the flow field. The Laplacian kernel in the flow-guided diffusion is deformed along the flow field as shown in Figure 2 (c). Flow-guided diffusion can be considered an arrangement factor. In Figure 2 (d), the patterns in flow-guided diffusion are arranged with the flow field but differ from those from regular kernels, which deform the shape of the pattern.

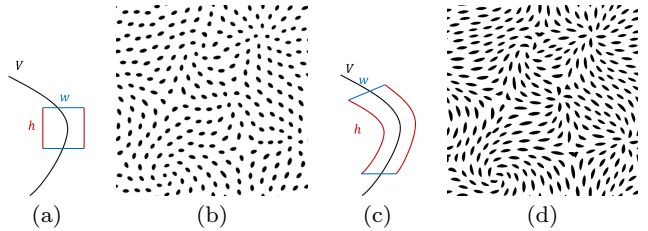


**Fig. 2** Comparison of different diffusion kernel. (a) Fixed and regular diffusion kernel. (b) Results with regular kernel in anisotropic diffusion. (c) Deformed diffusion kernel. (d) The patterns are rotated and deformed along the flow field in a flow-guided anisotropic diffusion.

##### 3.2.1 pattern stabilization

According to the Gray-Scott model, the diffusion rates  $D_A$  and  $D_B$  are usually set as 2:1 in isotropic diffusion. By using Eq. 2, the spot pattern generated by using the setting  $F = 0.0300$  and  $k = 0.0655$  is stable and regular in isotropic diffusion. However, this rule is broken

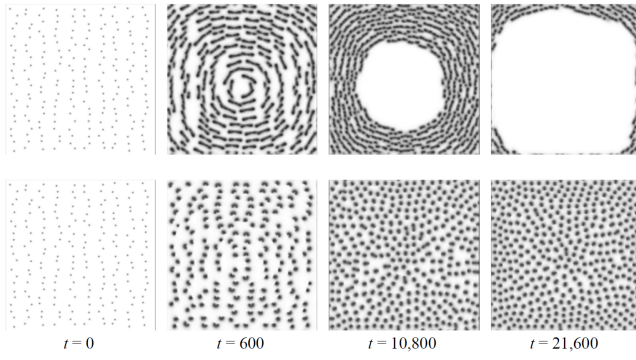


**Fig. 3** Comparison of stability in anisotropic diffusion;  $t$  is the iteration times. Top row: The resulting pattern is unstable when nonsymmetrical anisotropic diffusion is used. Bottom row: The resulting pattern is stabilized by applying the modified anisotropic diffusion. We use  $F=0.0300$  and  $k=0.0655$  (type  $\lambda$ : spot-like pattern) in both cases.

when the anisotropic diffusion is not a symmetric polar function. For example, with an anisotropic function specified as  $a(\theta) = \sin(0.5\theta)$ , the patterns are unstable and keep changing in anisotropic diffusion when various angles ( $a(\theta_{V,\nabla A})$  for  $A$ ,  $a(\theta_{V,\nabla B})$  for  $B$ ) are used, as shown in Figure 3. Thus, the anisotropic function is modified to ensure that the patterns will not only deform anisotropically, but will also maintain stability as in isotropic diffusion. The modified formula applied the  $a(\theta_{V,\nabla A})$  as anisotropic function for both A and B. According to the modified formula, we maintained the diffusion rate at 2:1 as the anisotropic functions are the same for each element. Therefore, the stable anisotropic pattern is obtained as shown in Figure 3 (bottom row).

### 3.2.2 Shape deformation

Kim and Lin [6] proposed the following diffusion term in discretized form:

$$\begin{aligned} \nabla \cdot (a(\theta) \nabla A) &\approx \frac{1}{D_{\eta(i)}} \sum_{j \in \eta(i)} \frac{1}{\|x_j - x_i\|} \frac{a(\theta_j) + a(\theta_i)}{2} (A_j - A_i) \\ a(\theta) &= \frac{m}{2} (1 + \cos(l(\theta + \theta_0))), \\ m = a_n, \text{ when } &\frac{(n-2)\pi}{l} < (\theta + \theta_0) \leq \frac{n\pi}{l} \end{aligned} \quad (3)$$

The effect of the distance to neighbor is reduced because the distance  $\|x_j - x_i\|$  is inversely proportional to the diffusion weight, and  $D_{\eta(i)}$  is the sum of the distance. The function  $a(\theta)$  in Eq. 3 is a general cosine-based anisotropy function where  $\theta_0$  denotes the rotation angle and  $l$  controls the edge number of the generated polygon pattern. The flow field  $V$  in these results contains outward flow from center. The detailed parameters are listed in Table 1.

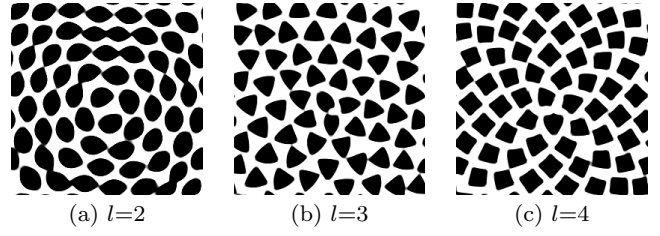


**Fig. 4** Spot patterns generated by the cosine-based anisotropy function in Eq. 3.

In addition, the users can also specify different anisotropic functions to different portions in polar coordinate. For example, Eq. 4 demonstrates an unsymmetrical pattern by setting the part in 0 to 180 degree to a constant. The water drop, hill-shape and sector patterns can be generated by the modified anisotropic functions in Figure 5.

$$a(\theta) = \begin{cases} 1, & \text{if } 0 \leq \theta + \theta_0 \leq \pi, \\ \frac{m}{2} (1 + \cos(l(\theta + \theta_0))), & \text{otherwise.} \end{cases} \quad (4)$$

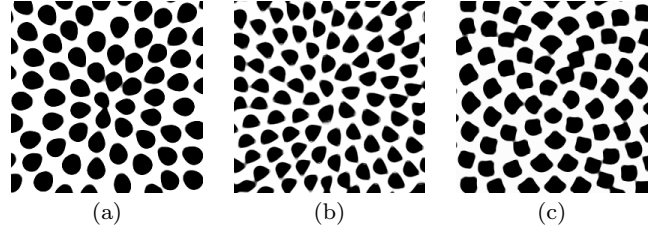


**Fig. 5** Stylized spot patterns generated by Eq. 4; (a) Water drop pattern; (b) hill shape; (c) sector pattern. The parameters for these two patterns can be found in Table 1.

**Table 1** Pattern style and control parameters.

Style	$a(\theta)$	$F$	$k$	$l$	Figure
spot: spindle	Eq. 3	.0375	.0655	2	Fig. 4(a)
hole: spindle	Eq. 3	.0300	.0546	2	Fig. 8 blue
stripe	Eq. 3	.0300	.0620	2	Fig. 8 green
triangle	Eq. 3	.0375	.0655	3	Fig. 4(b)
spot: quad	Eq. 3	.0375	.0655	4	Fig. 4(c)
water drop	Eq. 4	.0375	.0655	2	Fig. 5(a)
hill	Eq. 4	.0375	.0655	3	Fig. 5(b)
sector	Eq. 4	.0375	.0655	4	Fig. 5(c)

### 3.3 System workflow

To allow an effective design of the generated patterns from reaction diffusion, the shape and pattern arrangement for anisotropic reaction diffusion were considered.

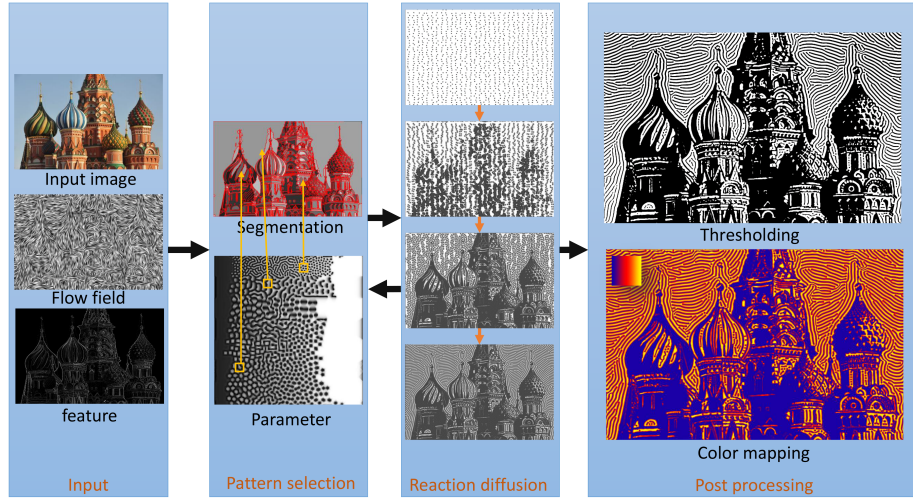


**Fig. 6** Flow chart of the proposed system.

As illustrated in Figure 6, the workflow of the proposed system consists of four main steps, *preprocessing*, *pattern selection and editing*, *reaction diffusion*, and *post-processing*. In preprocessing, the input image is converted into a flow field either by using the ETF or manually, according to the user's requirements. In pattern selection and editing, a control image is generated based on the salient features of the input image and user-specific parameters in order to guide the shape of the resulting reaction diffusion. Next, reaction diffusion is initialized using the input image, control image, and flow field. Multiple iterations are executed to automatically generate a density field. Iterations are conducted until the pattern is complete or stop by users. In post-process, the resulting density field from reaction diffusion is converted by using thresholding and color mapping to achieve a variety of artistic styles.

### 3.3.1 Preprocess

The visual cue of flow is generated from the input image by using the ETF [5]; subsequently, the pattern deformation and arrangement are controlled by modifying the flow field. We also extract the feature lines of the input image to continually add to the reaction diffusion process to keep these features in the final result.

### 3.3.2 Pattern selection and editing tools

In the proposed system, the pattern style can be controlled by the parameters  $F$ ,  $k$ , and  $l$ , and the pattern size is controlled by  $S_D$  and  $S_R$ . The main idea of providing an intuitive tool for users is to summarize these parameters into a single image called guiding image, as shown in Figure 7. The stable patterns in anisotropic reaction diffusion are encoded by the parameters

$k$  and  $l$  to provide an intuitive pattern picker for users. Users can choose a pattern and design their stylizations through the pattern picker.

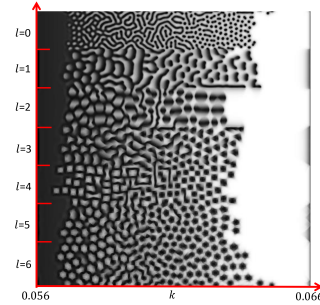


**Fig. 7** The guiding image summarized the patterns for  $F=0.0375$ . The  $x$ -axis denotes the parameter  $k$  ranging from 0.056 to 0.066, and  $y$ -axis represents the parameter  $l$ , ranging from 0 to 6. Various shape deformations are generated by anisotropic diffusion.

To specific local stylization, the input image is segmented into several regions. The regions can be assigned different control parameters. For instance, in Figure 8, given a flow field and a control image, and given the mapping between the control image and the pattern styles, a density field can be generated through the proposed system. The control image can be generated according to the tone of the input image or specified manually. In addition, the parameter in the control image can be edited in per pixel level, for example, a gradient tool for controlling size variation.

To generate a size scalable pattern, one common approach is to add the weight function to control the speed of the diffusion and reaction terms to control the size of the generated pattern.  $S_D$  and  $S_R$  denote the scalar weight function of the diffusion and reaction

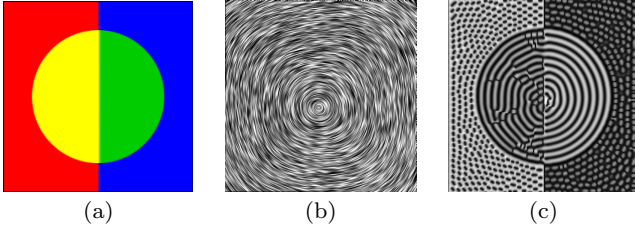


**Fig. 8** Pattern styles using the control image and flow field. (a) Control image. Each region is represented by colors and assigned a different set of parameters. In the example, red represents spot pattern, blue denotes hole, green represent line, and yellow denotes inverse line. (b) Flow field. (c) Patterns generated by settings in control images.

terms, respectively, and the pattern size is proportional to  $S_D/S_R$ ; the parameter space of  $S_D$  and  $S_R$  is shown in Figure 9.  $S_D$  and  $S_R$  have to be greater than 0 to avoid generating failure patterns.

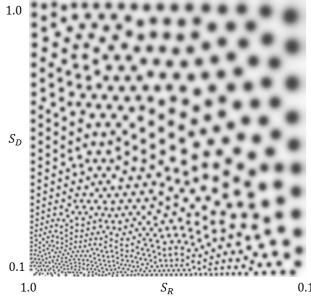


**Fig. 9** Size variation of the parameters of  $S_D$  and  $S_R$ .

### 3.3.3 Postprocessing

**Tone preserving thresholding.** The resulting density field is generally blurred with soft contour because of the nature of the diffusion process. Therefore, several image processing are performed to enhance the density field. First, the adaptive histogram equalization [13] is applied to the density field to ensure that the local maximum is more consistent. Second, thresholding is performed to segment the density field into patterns with clear shapes. However, the size of the pattern affected by a global thresholding value may not reflect the tones in the input image. To produce a tone-preserving pattern automatically, we split the histogram of the input image into several bins with equal size to compute appropriate thresholding values for each gray value as shown in Figure 10 (a) right. Each pixel in the density field is locally thresholded to black/white according to the thresholding values of the tone image, such that the pattern size is adjusted to match the tone map. Figure 10 describes how tone-preserving thresholding can be

used to transform the density field into patterns of a similar tone to the input image.

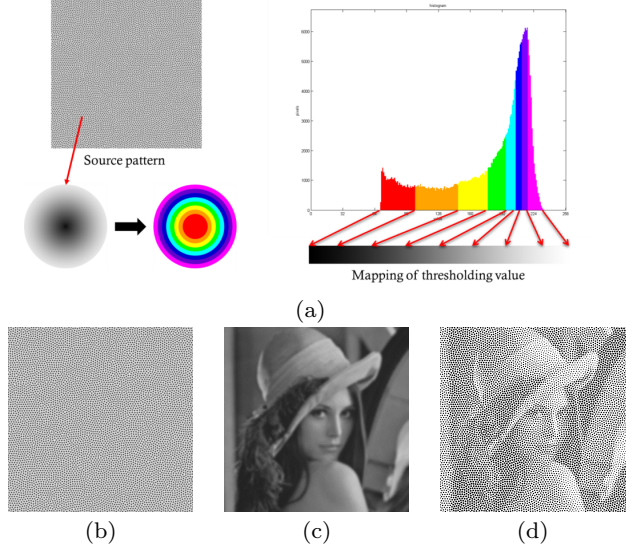


**Fig. 10** Thresholding process. (a) Relationship between the density distribution and histogram. A tone image (c) is mapped to several appropriate thresholding values by using clipping histograms; the density field (b) is transformed to a halftone result (d).

**Direction preserving color mapping.** Although desired patterns can be generated using parameter adjustment and thresholding, a single-channel density field in reaction diffusion limits color presentation. The idea of extended toon-shading [1] is used to express more visual cue, such as the direction and magnitude of the flow field and color of the input image. Extended toon-shading was used in a 2D texture map to encode both shading and viewing distance information for various shading effects. We adapt this multi-parameter information on a 2D map. Additionally, the 2D color mapping method provides flexibility in visual effects.

We parameterized the pattern space into polar angle coordinate. In our observation, the density value of pattern center is a local maximum because of the pattern grow from its center in reaction diffusion. Thus, the diffuse direction of the density field in the reaction diffusion can be expressed by the gradient of density field. We considered the distance from  $p_i$  to the center of the pattern to be the density value, and the angle between the flow direction  $v_f^i$  and gradient of density field  $v_g^i$ , as shown in Figure 11(c). The polar coordinate conversion for each pixel  $p_i$  is then given by

$$\begin{aligned} r_i &= A(p_i) \\ \theta_i &= \cos^{-1}\left(\frac{v_f^i \cdot v_g^i}{|v_f^i||v_g^i|}\right) \end{aligned} \quad (5)$$

where  $[r_i, \theta_i]$  denotes the radius and angle in the polar coordinate, and  $v_f^i$  and  $v_g^i$  denote the gradient vector of density field and direction vector of flow field for each pixel  $p_i$ , respectively.

The proposed polar coordinate representation is useful to visualize flow directions. We can extend it with motion illusion. Motion illusions are still images that contain special repeated asymmetric patterns for evoking illusory motion. The most used repeated asymmetric pattern is black-blue-white-yellow. Chi et al. [3] proposed a method to place repeated asymmetric patterns to create self-animating images. Based on this concept, the repeated asymmetric pattern is encoded in the polar coordinates, as shown in Figure 11(a). The polar coordinate is divided into three main regions according to radius: high-, middle-, and low-density. The high-density region is painted blue whereas the low-density region is painted yellow. The middle region was separated into two subregions are painted to black or white according to the angle alone the vector field. Figures 11(b) and (c) show the density field converted into a still image with motion illusion to depict a flow direction with Eq. 6;  $C_i$  is the color of pixel  $i$ ;  $r_{min}$  and  $r_{max}$  are the range of the middle regions.

$$C_i = \begin{cases} \text{yellow} & \text{if } r_{max} < r_i < \infty \\ \text{black} & \text{if } r_{min} < r_i < r_{max} \text{ and } 0 < \theta_i < \pi \\ \text{white} & \text{if } r_{min} < r_i < r_{max} \text{ and } \pi < \theta_i < 2\pi \\ \text{blue} & \text{if } 0 < r_i < r_{min} \end{cases} \quad (6)$$

## 4 Experimental results

The goal of the proposed paper is to provide various patterns to design stylized images and provide an intuitive system to help users to choose patterns and design stylized result. First, we demonstrated several kind of stylized results include paper cutting, stylized halftoning, and flow visualization with illusory motion. Second, we conducted user study to demonstrate the feasibility of the proposed system and collected feedback from users.

### 4.1 Image stylization

#### 4.1.1 Paper-cut art

Paper cut art comprising the repetition of patterns with clearly arranged shapes along the flow field, is a type of image stylization. In Myriam Dion's paper cut artworks, images from newspapers are taken as the input;

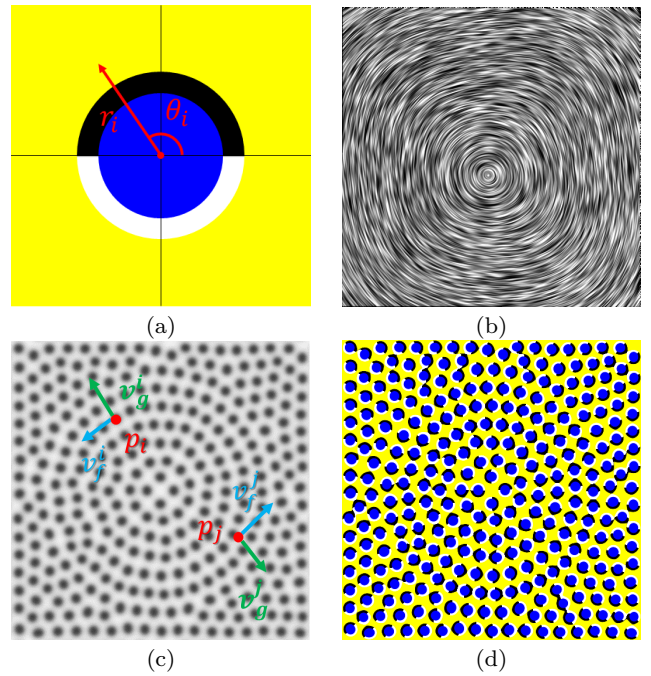


**Fig. 11** Motion illusion using color mapping. (a) Color map in polar coordinate; (b) flow field; (c) density field generated by reaction diffusion; (d) the mapping result can evoke motion illusion. The effect will be stronger when zoom in the image.

the flow direction is visualized by hollowing image using directional and closely arranged patterns. In our system, the direction and arrangement of the patterns can be controlled by modifying the flow field. By generating a black-and-white pattern, the user can create images in the paper cut style. Figure 12 shows a simple case of paper cut art with a quad pattern arrangement in the flow field. A starry night demonstrates a complex paper-cut in Figure 13; the flow-guided spindle patterns are used to replace the sky and distinguished the regions of clouds, stars, and the moon by different arrangement and deformed parameters. Figure 14 demonstrates another complex case with multiple stylized patterns: the size of the pattern is enlarged from the center to the border to enhance the visual effects of the blooming flowers.

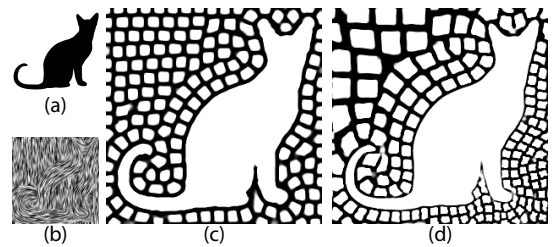


**Fig. 12** Simple paper cutting. (a) Input image; (b) flow field; (c) result with thresholding, and (d) result with size gradient control.

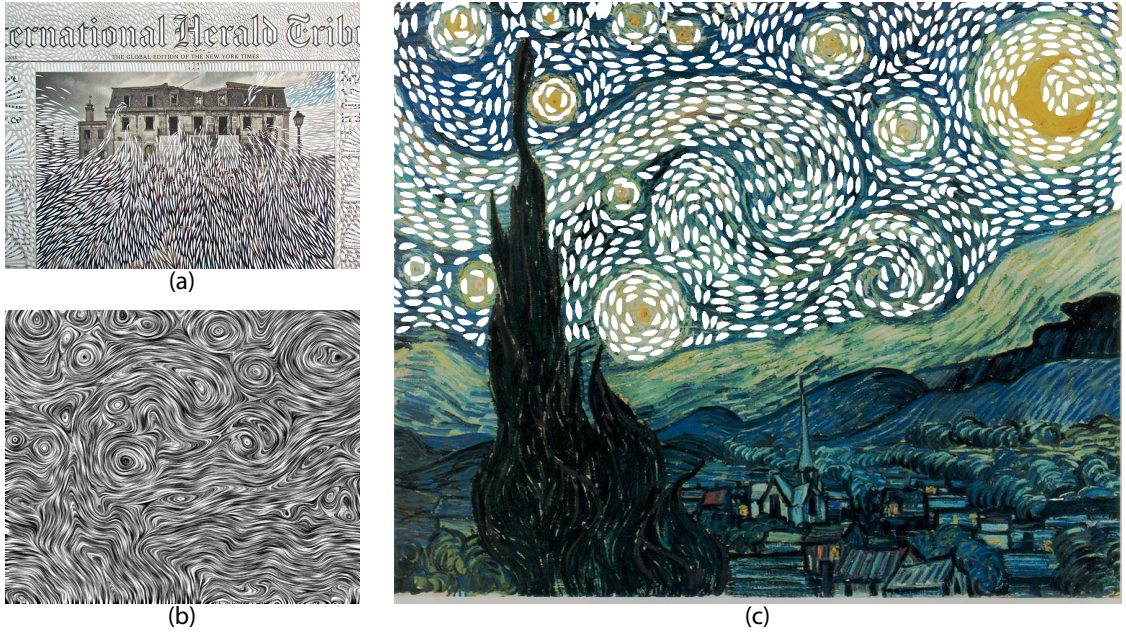


**Fig. 13** Complex paper-cut images. (a) Paper-cut artwork by Myriam Dion; (c) our result (*Starry Night*) using the flow field (b).

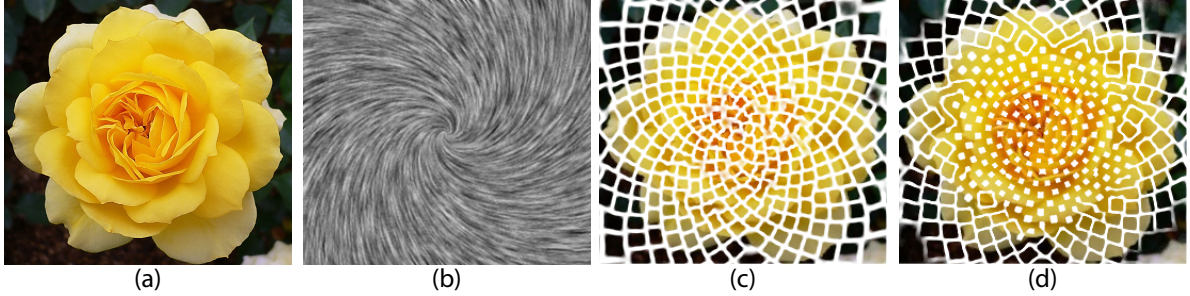


**Fig. 14** Complex paper-cut art. (a) Source image; (b) vortex flow; (c) result with gradient size control; (d) result with gradient size and pattern type control, pattern size and type will change according the distance to center.

#### 4.1.2 Stylized halftone images

The proposed method also can create stylized halftone images. In Marcos Marin's stylized halftone artwork, portrait photographs are taken as the input images, then the feature of images were replaced by line-type patterns. To express the luminance of the input image, the thickness of line patterns is mapped by the level of luminance; thus, the completed artworks become stylized halftone images or optical artworks. We use thresholding method to transform the anisotropic spot pattern into a stylized halftone image, as shown in Figure 15. A more complex case of the stylized halftone style with optical art effects is shown in Figure 16. In addition to the single-pattern style, our system also enables multiple patterns to be specified in segmented images. For segmented images, different parameters are

assigned to each region to generate multiple patterns in the image shown in Figure 17.

#### 4.1.3 Flow field visualization

In addition to image stylization, our method enables flow visualization. To visualize flow-field information, we specify control factors in regard to the orientation and magnitude of the flow field. Patterns deformed by anisotropic diffusion can indicate the orientation of the flow field, and the pattern size can provide an intuitive map to the magnitude. In our results shown in Figure 18, the magnitude of the flow field is indicated by the deformed circle along the flow direction. Compared with the results of Sanderson et al. [14], the proposed color mapping method facilitated generating the motion illusion effect. Figure 19 shows an alternative color mapping method used to convert the density field into

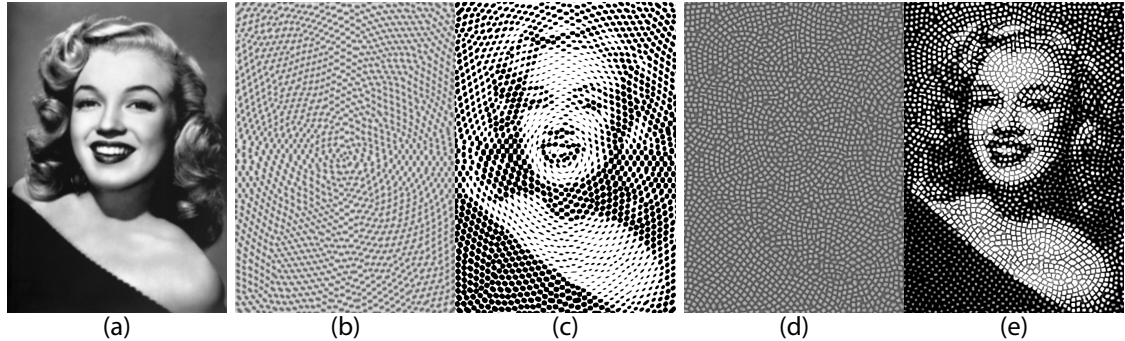


**Fig. 15** Halftone image with thresholding control. (a) is reference tone image. The pair of (b) and (c) are density field and thresholding result with vortex flow field and spindle spot pattern. The pair of (d) and (e) are density field and thresholding result with the ETF of (a) and hole pattern.

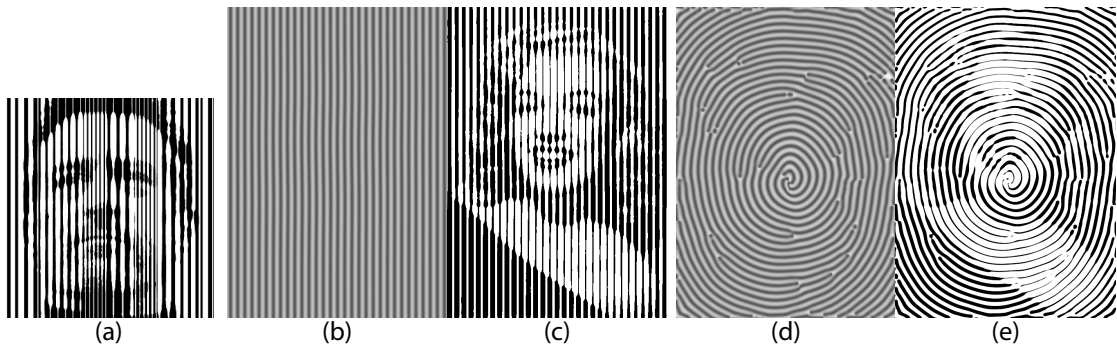


**Fig. 16** Stylized halftone images inspired by Marcos Marin's artwork (a). (b) and (d) are density fields were generated with straight flow field and vortex (c) flow fields, separately. And (c) and (e) are the halftone image by applying the tone preserving thresholding from (b) and (d).

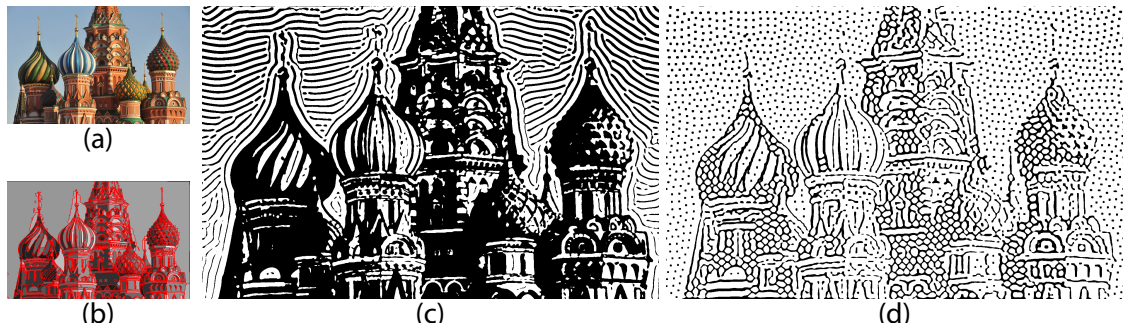


**Fig. 17** Stylized halftone images featuring multiple patterns. (a) Input image; (b) segmentation result; (c) stylization result by using black, white, and line patterns; (d) stylization result by using quad-spot and hole patterns.

a quad/triangle pattern; because reaction diffusion is self-organizing, a favorable pattern distribution is obtained automatically.

#### 4.2 User study

A user study involving 14 participants, aged 20 to 30 years, was conducted to evaluate the proposed method. In the user study, we compared the completion time in the design process using the functions of slider bar and pattern picker, 10 minutes for freely creation, and we

collected the feedbacks from users. The study begins with a 10-minute introduction to the anisotropic reaction diffusion, the user study, and the interface. The participants were asked to complete the defined task. For given image and flow field, they are asked to use the proposed system to design a stylized similar to the target image. We use Figure 12(a) and Figure 12(c) as the input and target image in the task. The participants are grouped into teams A and B. The team A uses pattern picker only to complete the tasks. The team B carries out the task using a slider bar only with the informa-

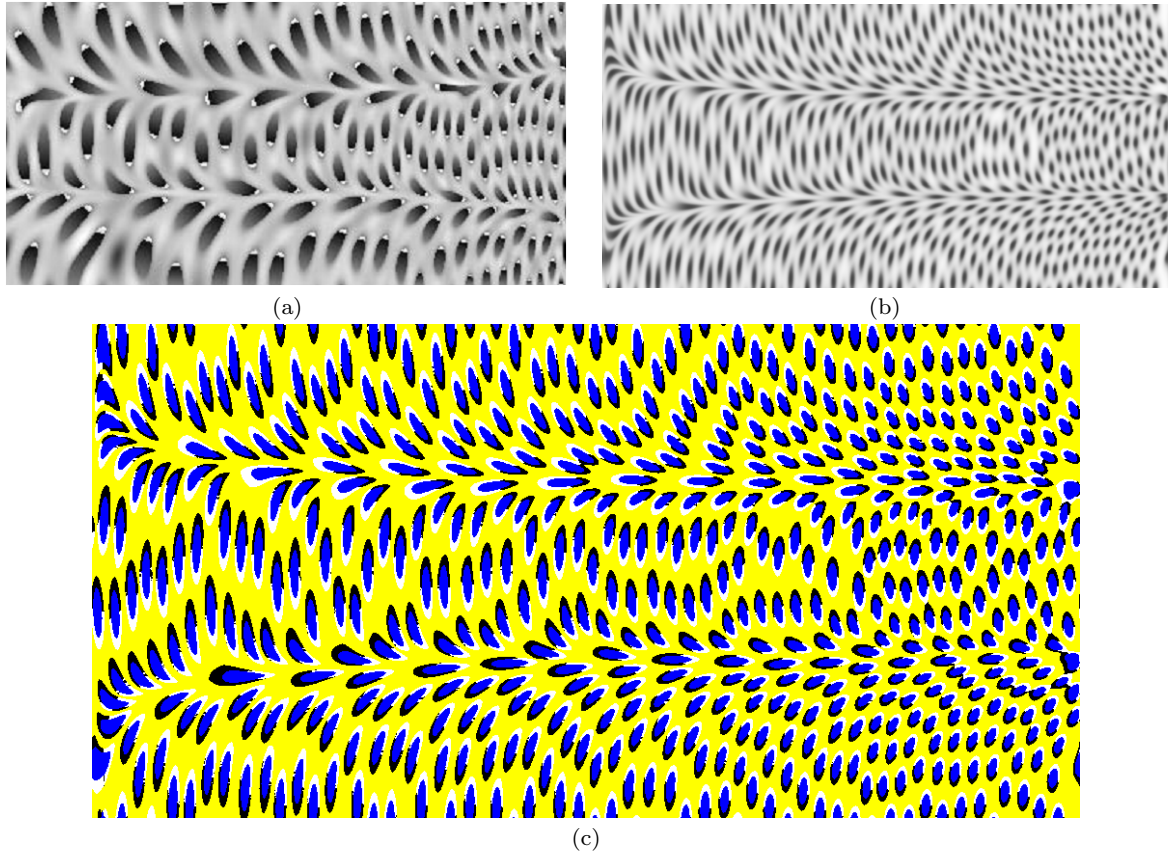


**Fig. 18** Flow visualization comparison. (a) is from Sanderson et al. [14]; our method is shown in (b), in which a density field generated by reaction diffusion is depicted; (c) shows motion illusion by using color mapping.

tion in Table 1. After the predefined task, participants are asked to freely create images in 10 minutes. Finally, participants are asked to evaluate the results and to judge the artist work and our result in Figure 13 and Figure 16, in terms of style similarity and aesthetic of shape and arrangement. The results randomly appear in screen, without any label to hide which one is created by artist. The user study lasted approximately 50 minutes for each participant.

By comparing Team A and B, we can find that the average completion time using a pattern picker is obviously less than the time using a slider bar (195 seconds vs. 396 seconds). These survey results show that the pattern picker is more intuitive, in terms of desired pattern selection, than the parameter selection. The results created by users are shown in Figure 20. The variety of results supports the feasibility of the proposed system. Table 2 shows the user survey result, which indicates that most people agree the results of proposed system have good pattern arrangement (avg.=3.62), variety in patterns (avg.=3.77), and pattern shape (avg.=3.62). From Figure 21, 50% and 86% of the participants agree that our results are similar to the artist' styles (paper cutting and stylized halftone), respectively. Figure 22

shows that 78.5% and 71% of the participants agree our results are more aesthetic than the artist. The result is beyond our expectation, it may due to aesthetic is subjective or the starrynight and Marilyn Monroe are famous and eye-catching.



**Fig. 20** Gallery of results created by users.

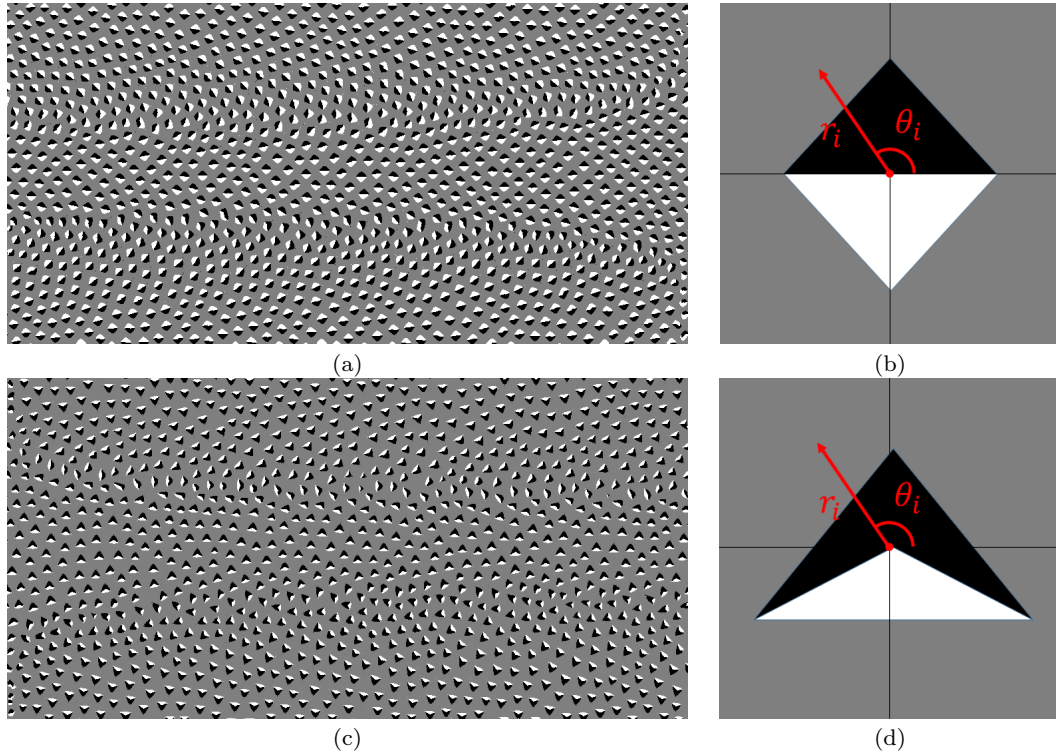


**Fig. 19** Flow visualization. Quad (a) and triangle (c) spot patterns were generated by using the color mapping in polar coordinate shown in (b) and (d).

**Table 2** Result of the questionnaire survey. Score from 1 (min) to 5 (max).

Question	Average	SD
Q1. Aesthetic in pattern arrangement	3.62	0.84
Q2. Variety of pattern type	3.77	0.8
Q3. Aesthetic in pattern shape	3.62	0.92

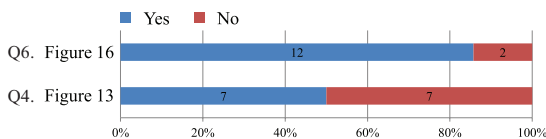


**Fig. 21** Result of the questionnaire survey. Are two styles the same? for Figure 13(papercut) and Figure 16(halftone).

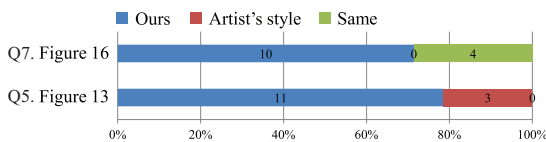


**Fig. 22** Result of the questionnaire survey. Which is better in aesthetic? for Figure 13(papercut) and Figure 16(halftone).

### 4.3 Performance

The proposed method was implemented using C++ and OpenCV. All experiments were evaluated on a PC with a 3.4 GHz CPU and nVidia geforce GTX 670. The main computational bottleneck in the reaction diffusion is

the calculation of the modified diffusion term, which is an iterative process. In our implementation, GPU computing is adopted to speed-up this step.

Our system takes 4 to 30 seconds to generate a stable result in 50,000 iterations. The image resolution is independent of the number of iterations. To demonstrate the feasibility of the proposed method, various patterns were tested. and the results were compared with artist-made works.

**Table 3** Computing performance. Time denotes the time to stable pattern

Resolution	FPS (CPU)	FPS (GPU)	Time on GPU
256×256	62	2,210	4.5s
512×512	18	1,311	7.6s
1024×1024	4	323	30.9s

### 5 Conclusions and future work

This study proposes an anisotropic pattern generation method for image stylization. The method integrates flow fields and anisotropic reaction diffusion. The core algorithm is created by extending the reaction diffusion model; the proposed method offers a pattern picker to choose stylized patterns and avoid complex parameters

adjustment. Consequently, it can be used to produce images in various styles. In addition, thresholding and color mapping are proposed to design the density distribution and color to preserve the feature of input image and flow field. The self-organizing properties of reaction diffusion permit a less regular pattern; thus, the results resemble handmade images. The effectiveness of the proposed system was confirmed by applying the system to create images in paper cut and stylized halftone styles.

In the future, the authors extend the proposed method to include surface and volume data. However, this approach requires meeting the challenge of redefining the anisotropic Laplacian kernel on the 3D domain and reducing the costs of complex computation. Furthermore, the method may be integrated with additional reaction diffusion models and extended to produce a greater variety of patterns. The system has certain limitations. For example, when the flow field was discontinuous, the generated patterns became noisy and broken. Moreover, because the generated patterns were obtained by deforming patterns resulting from reaction diffusion, the method might have certain natural limitations in generating certain complex patterns, for example, snowflake patterns. We also aim to explore an inverse process to optimize the parameter, initial density distribution, and flow design of reaction diffusion system to reproduce a given pattern.

**Acknowledgements** We would like to thank the anonymous reviewers and the editor for their valuable comments. This work is supported by the ministry of science and technology, Taiwan under MOST 103-2221-E-004-008.

## References

1. Barla, P., Thollot, J., Markosian, L.: X-toon: An extended toon shader. In: Proceedings of the 4th International Symposium on Non-photorealistic Animation and Rendering, NPAR '06, pp. 127–132. ACM, New York, NY, USA (2006)
2. Bousseau, A., Neyret, F., Thollot, J., Salesin, D.: Video watercolorization using bidirectional texture advection. In: ACM SIGGRAPH 2007 Papers, SIGGRAPH '07. ACM, New York, NY, USA (2007)
3. Chi, M.T., Lee, T.Y., Qu, Y., Wong, T.T.: Self-animating images: illusory motion using repeated asymmetric patterns. In: ACM Transactions on Graphics (TOG), vol. 27, p. 62. ACM
4. Kang, H., Lee, S., Chui, C.K.: Coherent line drawing. In: Proceedings of the 5th International Symposium on Non-photorealistic Animation and Rendering, NPAR '07, pp. 43–50. ACM, New York, NY, USA (2007)
5. Kang, H., Lee, S., Chui, C.K.: Flow-based image abstraction. IEEE Transactions on Visualization and Computer Graphics **15**(1), 62–76 (2009)
6. Kim, T., Lin, M.: Stable advection-reaction-diffusion with arbitrary anisotropy. Comput. Animat. Virtual Worlds **18**(4-5), 329–338 (2007)
7. Kyprianidis, J.E., Döllner, J.: Image abstraction by structure adaptive filtering. In: Proc. EG UK Theory and Practice of Computer Graphics, pp. 51–58 (2008)
8. Kyprianidis, J.E., Kang, H.: Image and video abstraction by coherence-enhancing filtering. Computer Graphics Forum **30**(2), 593–V602 (2011). Proceedings Eurographics 2011
9. Lee, H., Seo, S., Ryoo, S., Yoon, K.: Directional texture transfer. In: Proceedings of the 8th International Symposium on Non-Photorealistic Animation and Rendering, NPAR '10, pp. 43–48. ACM, New York, NY, USA (2010)
10. Li, Y., Bao, F., Zhang, E., Kobayashi, Y., Wonka, P.: Geometry synthesis on surfaces using field-guided shape grammars. Visualization and Computer Graphics, IEEE Transactions on **17**(2), 231–243 (2011)
11. McGraw, T.: Generalized reaction diffusion textures. Computers & Graphics **32**(1), 82–92 (2008)
12. Pearson, J.E.: Complex patterns in a simple system. Science **261**(5118), 189–192 (1993)
13. Pizer, S.M., Amburn, E.P., Austin, J.D., Cromartie, R., Geselowitz, A., Greer, T., Romeny, B.T.H., Zimmerman, J.B.: Adaptive histogram equalization and its variations. Comput. Vision Graph. Image Process. **39**(3), 355–368 (1987)
14. Sanderson, A.R., Johnson, C.R., Kirby, R.M.: Display of vector fields using a reaction-diffusion model. In: Proceedings of the Conference on Visualization '04, VIS '04, pp. 115–122. IEEE Computer Society, Washington, DC, USA (2004)
15. Son, M., Lee, Y., Kang, H., Lee, S.: Structure grid for directional stippling. Graphical Models **73**(3), 74–87 (2011)
16. Steidl, G., Teuber, T.: Anisotropic smoothing using double orientations. In: Scale Space and Variational Methods in Computer Vision, pp. 477–489. Springer (2009)
17. Turk, G.: Generating textures on arbitrary surfaces using reaction-diffusion, vol. 25. ACM (1991)
18. Wan, L., Liu, X., Wong, T.T., Leung, C.S.: Evolving mazes from images. Visualization and Computer Graphics, IEEE Transactions on **16**(2), 287–297 (2010)
19. Witkin, A., Kass, M.: Reaction-diffusion textures. ACM Siggraph Computer Graphics **25**(4), 299–308 (1991)
20. Xu, J., Kaplan, C.S.: Artistic thresholding. In: Proceedings of the 6th International Symposium on Non-photorealistic Animation and Rendering, NPAR '08, pp. 39–47. ACM, New York, NY, USA (2008)
21. Xu, J., Kaplan, C.S., Mi, X.: Computer-generated papercutting. In: Proceedings of the 15th Pacific Conference on Computer Graphics and Applications, PG '07, pp. 343–350. IEEE Computer Society, Washington, DC, USA (2007)
22. Zang, Y., Huang, H., Li, C.F.: Artistic preprocessing for painterly rendering and image stylization. The Visual Computer **30**(9), 969–979 (2014)